Experimental Evaluation of a Residential Refrigerator with a Novel Rotating Heat Exchanger as an Evaporator

Viral K. Patel , Anne Mallow, Ayyoub Mehdizadeh Momen, Terry Johnson, Wayne Staats, Omar Abdelaziz

ABSTRACT

Residential refrigerator designs have improved significantly over the recent years to achieve the required federal minimum energy standard and match with consumer expectations. Designers have been able to use innovative design features and components; however, evaporator designs have lagged in performance improvement due to the need to properly manage frost and maximize the freezer interior volume. Rotating Heat Exchangers (RHX) provide an innovative solution that addresses both of these concerns. The rotation of the fins results in continuous disruption to the boundary layer, hence reducing the overall thermal resistance. Thus, for the same capacity, the heat transfer area can be greatly reduced. Furthermore, the rotation inhibits frost growth on the fins and reduces the time and frequency of defrosting. In this paper, we present an experimental evaluation of the RHX in a benchtop refrigerant loop system showing results for different operating configurations. Cooling capacity, cooling COP, and overall energy consumption are investigated. High-speed imaging is also used to capture frost growth patterns over time on the RHX fins in the presence and absence of rotation. The results show that the rotating heat exchanger evaporator is capable of meeting the 100 W capacity requirement of residential refrigerators, while offering the potential of significant reduction in defrost energy consumption.

Introduction

The operation of home appliances such as refrigerators, clothes washers, and dryers contributes to approximately 16% of household electricity use (EIA 2009). Refrigerators, in particular, are found in nearly all homes in the US. Due to the implementation of federal standards (DOE 2012) since 1987, their efficiency has significantly improved, and corresponding energy consumption has reduced from 1000 kWh/year to less than 500 kWh/year (Mauer et al. 2009). However, there is still room for improvement as new standards aim to further increase efficiency, and programs to facilitate the adoption of high-efficiency appliances are expanded (York et al. 2015). At the component level, energy use in a refrigerator can be lowered by improving insulation, using more efficient compressors, using advanced control schemes and improved heat exchanger design. The research presented in this paper mainly focuses on improved heat exchanger design.

Heat exchangers used in space conditioning systems are limited by the low air-side heat transfer. To increase the air-side heat transfer surface area, extended surfaces such as fins are commonly incorporated. Examples include finned heat sinks in electronics cooling, vehicle radiators, and fin and tube evaporators for household refrigeration. They are typically used with an electrical fan that promotes air circulation and convective heat transfer. For household refrigeration applications, limitations on fan size and noise results in inadequate airflow to prevent or delay frost growth on the evaporator fins. Eventually, a large amount of frost forms, which negatively impacts the performance of the heat exchanger. Frost results in an increased pressure drop between fins which reduces or even completely blocks airflow. It also creates an additional thermal resistance. To remove the frost layer, the freezer must undergo a defrost cycle. The length and frequency of defrost cycles (which often use high-powered electric-resistance heaters) significantly affect the overall energy consumption of the refrigerator. Therefore, a primary design objective of next-generation high-performance heat exchangers in refrigeration applications is to increase the air-side heat transfer coefficient, while minimizing the defrost time and frequency. One innovative way to achieve this is by setting the finned surface itself into constant motion, which increases the local air velocity in the vicinity of the fins and continuously disrupts the boundary layer.

Studies in frost formation on traditional fin and tube evaporators show that defrosting is inefficient; only 20% of heat supplied to the defrost heaters is useful in the removal of frost (Knabben, Hermes, and Melo 2011). The remainder causes the freezer compartment temperature to rise, increasing the load on the system. Therefore, minimizing the need to defrost or completing defrost cycle in a short time can have a favorable impact on the overall energy consumption of the system. While many recent experimental (da Silva, Hermes, and Melo 2011) and modeling (Cui et al. 2011; Hwang and Cho 2014) studies have been conducted on frost formation in fin and tube evaporators, this information is not available for rotating heat exchangers, which are a relatively new technology. There is, therefore, a necessity to fully characterize the operation of rotating heat exchangers and to study frost formation and its effect on performance. The work presented in this paper demonstrates the use of a rotating heat exchanger as a replacement for the current aluminum fin and tube evaporator in household refrigeration applications. It is installed in a controlled refrigeration cycle to study the performance in terms of ability to meet the capacity required by a typical household refrigerator and frost formation, growth and management during operation. The results of this first prototype evaluation will be used to inform the design decisions for the next generation prototype rotating heat exchanger.

Experimental Setup

Rotating heat exchanger evaporator

The air bearing heat exchanger, also referred to as a rotating heat exchanger (RHX), was first developed by Sandia National Laboratories to serve as a high-performance cooler. This heat exchanger has been shown to have extremely low thermal resistance, near silent operation, and has the potential for significant size reduction (Johnson et al. 2013; Staats et al. 2014). The RHX is a motor-driven, rotating, finned heat exchanger that consists of three main components: one or two impellers (a rotating, finned heat sink), a micro-channel baseplate, and integrated brushless DC motor(s) as shown in the cutaway solid model in Figure 1. For the work presented in this paper, a special design of the RHX with two 5.5” (140 mm) diameter aluminum impellers are

studied. Each impeller is powered by a motor and rotates over a gap on a stationary baseplate supported by an air bearing. Refrigerant flows through the baseplate (a 3-path design with 90 micro-channels, each 0.8 mm thick and 0.8 mm deep) while the moving fins pull air through the impellers, cooling it by transferring heat to the refrigerant through the impeller fins, impeller bases, air bearing gap (0.01 mm), and baseplate. Due to the rotation of the impeller fins at up to 1500 RPM, the air flow experiences a continual boundary layer disruption leading to an order of magnitude thinner boundary layer compared to conventional finned surfaces. As a result, the air-side heat transfer coefficient is greatly enhanced.

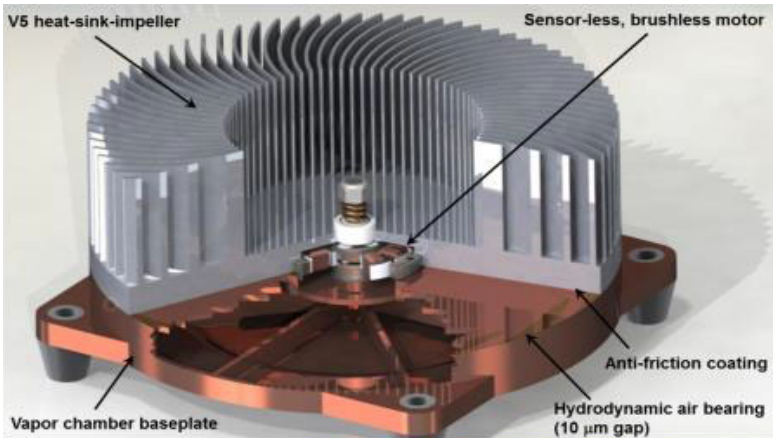

Figure 1: Cutaway diagram showing rotating heat exchanger assembly

Benchtop refrigerant loop

The rotating heat exchanger evaporator was installed in a benchtop refrigerant loop testing system to simulate conditions in a typical freezer compartment. The 124L test compartment was insulated with 3” (76.2 mm) of polyurethane. It had several conduits for electrical connections and viewing ports for a high-speed camera system. The insulated box was installed on top of a movable cart, and all other components of a vapor-compression cycle were installed below it on the bottom shelf. A schematic of the experimental setup is shown below in Figure 2.

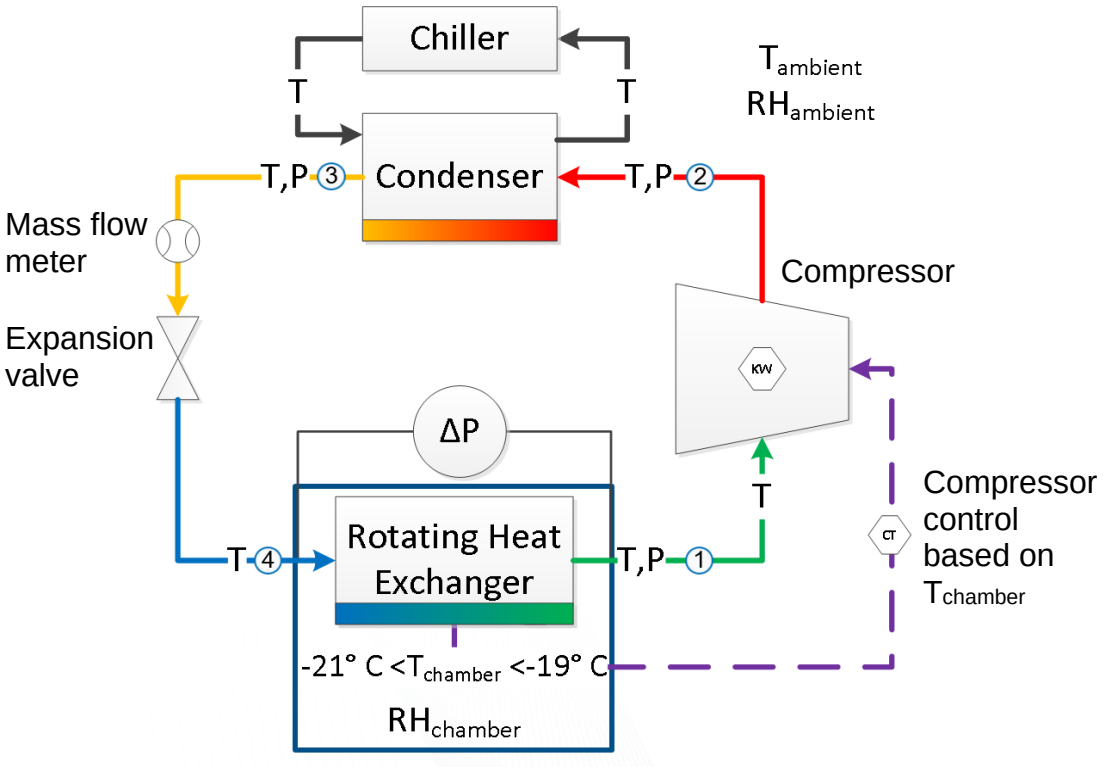

Figure 2: Schematic of benchtop refrigerant loop with RHX evaporator located in insulated box (auxiliary fan not shown)

The vapor-compression loop consisted of a compressor, tube-in-tube condenser (with recirculating chilled water as the coolant), expansion valves and connecting tubes. The working fluid in the cycle was refrigerant R134a. A Coriolis mass flow meter was used to measure refrigerant flow rate in the main loop. As shown in Figure 2, absolute and differential pressure transducers were installed at various points in the cycle. T-type, probe thermocouples were used for measuring the temperature of the refrigerant, and cooling water throughout the cycle, as well as air in the insulated box. Relative humidity sensors were installed both inside and outside the insulated box. A Watt transducer was used to measure compressor power consumption. A data acquisition system was used with LabVIEW software to measure and record data. LabVIEW was also used to provide a signal for thermostatic control of the compressor, based on the chamber temperature setpoint. The maximum systematic uncertainty of measured and derived quantities is given in Table 1 below.

Table 1. Maximum uncertainty for measured quantities

Measurement	Maximum uncertainty
Temperature (°C)	± 0.5°C
Absolute pressure, discharge (kPa)	± 1.72 kPa
Absolute pressure, suction (kPa)	± 0.172 kPa
Differential pressure (kPa)	± 0.172 kPa
Refrigerant mass flow rate (g/s)	± 0.1 %
Relative humidity (%)	± 0.8 %
Compressor power (W)	± 5.0 W
Derived quantity	Maximum uncertainty
Evaporator capacity (W)	± 0.76 W
COP	± 0.015

Figure 3 shows an image of the RHX impeller/baseplate combinations installed on the bottom of the insulated box.

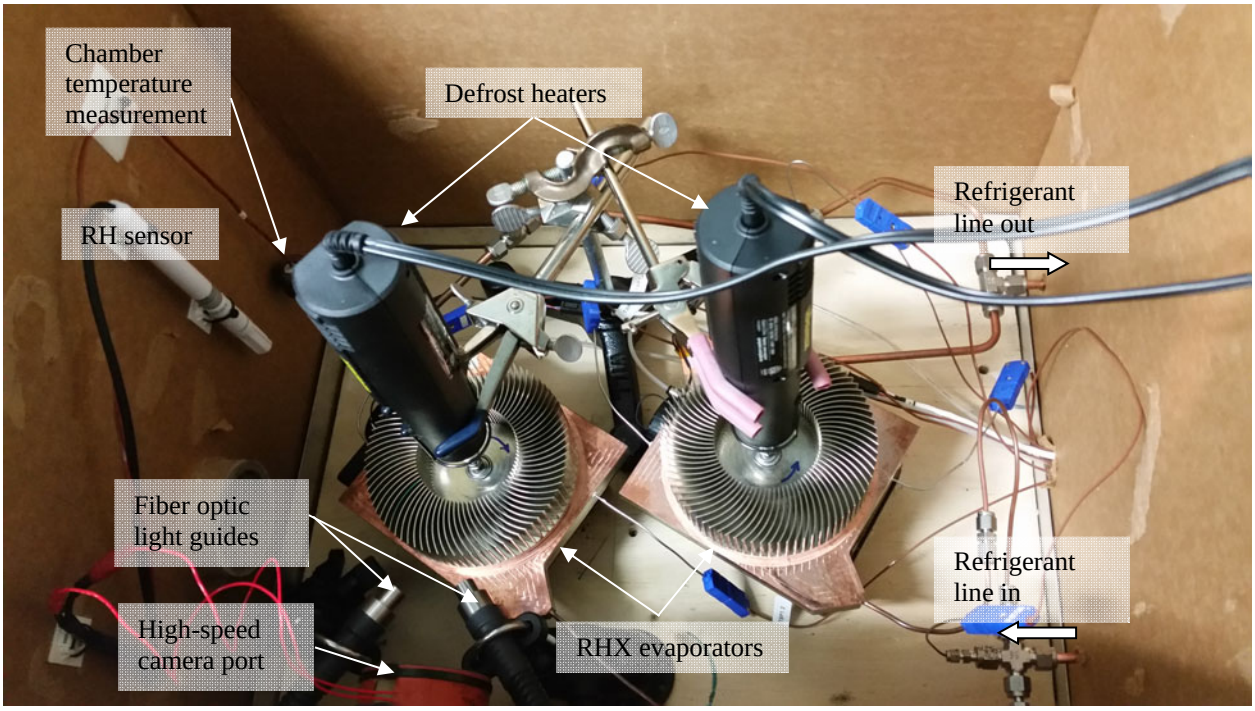

Figure 3: Installation of RHX evaporators in insulated box (auxiliary fan not shown)

High-speed imaging system

For imaging of frost formation on the rotating impeller fins, an Olympus i-SPEED3 camera system was used, along with a Navitar Optix 12x zoom lens. Two Edmund Optics DC-regulated illuminators with flexible fiber optic light guides provided high-intensity, localized light sources in the vicinity of the impeller fins. These were necessary for the high frame rates and shutter speeds required: the typical frame rate for image capture during rotation of the impeller fins (at rotational speed of ~1200 rpm) was 2000 fps with a shutter setting of 50x. The camera was mounted on a tripod situated at the side of the insulated box. The lens could be

focused by moving the camera into and out of the viewing port which was installed in the side wall of the box. The viewing port had a quartz glass window to maintain optical clarity. Using this configuration, several fins could be imaged at once, with the image covering their entire height, as will be shown in the next section.

Experimental results and discussion

The experiment procedure involved first closing and sealing the insulated box and starting the rotating impeller. The compressor was started and the expansion valve on the main loop was adjusted to achieve the desired conditions. The box was allowed to cool to a setpoint of -20°C (with ±1°C hysteresis). A relay was used for simple on/off control of the compressor. The evaporator capacity was determined using the mass flow rate and enthalpy change of refrigerant. Using the numbering of state points in Figure 2, the enthalpy at point 4 (evaporator inlet) was the same as the enthalpy at point 3 (condenser outlet), since the expansion process across the valve was assumed to be isenthalpic. The enthalpy at point 3 was determined from the pressure and temperature measurement since the refrigerant was subcooled as it exited the condenser. Similarly, the enthalpy at point 1 (evaporator outlet/compressor inlet) was determined from the pressure and temperature measurement, since the refrigerant was superheated as it exited the evaporator. These assumptions were validated during the experiment by programmatically exporting pressure and temperature measurements from the LabVIEW environment into NIST REFPROP (Lemmon, Huber, and McLinden 2013) software which allowed real-time determination of the thermodynamic state of the refrigerant.

Experiments in performance characterization and frost-formation for the double-impeller RHX evaporators were performed. Four different operating conditions were investigated:

1. Impellers on, auxiliary fan off
2. Impellers cycling on/off, auxiliary fan off
3. Impellers off, auxiliary fan on
4. Impellers off, auxiliary fan off

For experiment 2, the on/off cycling of the impellers was determined by the cycling of the compressor, based on the -20°C chamber temperature setpoint defined above. An auxiliary fan was installed in the insulated box for air circulation (as these are typically used alongside fin and tube evaporators in extant freezer compartments of household refrigerators). The auxiliary fan was only run for experiment 3, when the impellers were stationary. For each experiment, the heat loss rate, recovery rate, coefficient of performance and energy consumption were determined and compared. The experiments were performed in succession over the period of 4 days (24 hours per experiment) to minimize variation in refrigerant charge and mass flow rate.

The insulated box temperature (referred to as chamber temperature), evaporator capacity and compressor power for all four experiments are shown in Figure 4 over a period of 4 hours when steady-state conditions were reached.

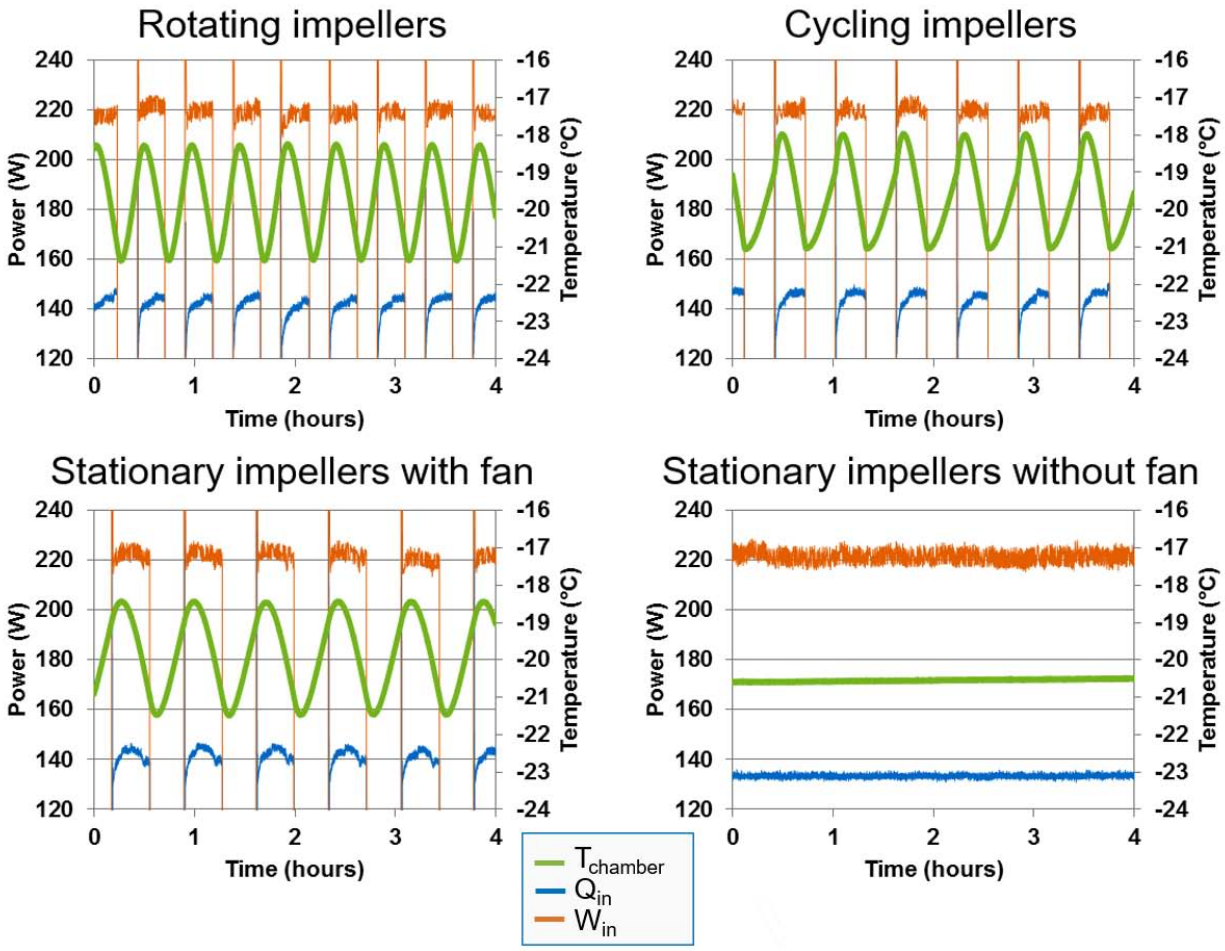

Figure 4: Chamber temperature, evaporator capacity (Q_{in}) and compressor power (W_{in}) for all experiments over 4 hours

As shown in the graphs above, the minimum setpoint temperature was reached in all experiments. However, the compressor did not cycle in experiment 4 as the lowest chamber temperature achieved was within the setpoint hysteresis (i.e. the temperature was never <-21°C at steady state). This meant that the compressor was continuously operating for the entirety of the experiment, which represented the most energy-intensive condition. For experiments 1-3, the frequency of compressor cycling was affected by the associated recovery rate and heat loss rate (defined as the rate of change of chamber temperature during compressor on and off periods, respectively). These were a function of the box insulation and air flow rate (produced via impellers or auxiliary fan). A summary of the above measurements averaged over the 4 hour period is given in Table 2, along with associated heat loss and recovery rates. The coefficient of performance was defined as the quotient of the evaporator capacity and compressor power.

Table 2: Average performance characterization of all experiments

Experiment #	Impeller status	Auxiliary fan status	Evaporator capacity, Q_{in} (W)	Compressor power consumption (W)	COP	Average heat loss rate* (°C/s)	Average recovery rate* (°C/s)
1	On	Off	137.3	225.0	0.616	0.0028	0.0035
2	Cycling	Off	140.5	225.1	0.628	0.0019	0.0035
3	Off	On	139.5	227.0	0.614	0.0016	0.0024
4	Off	Off	133.4	221.5	0.602	-	-

*Averaged over 4 cycles

As shown in Table 2, the differences in COP between experiments were minimal since the evaporator capacity and compressor power consumption were similar for all experiments. The objective of the current work was to demonstrate viability of using an RHX as an evaporator in a freezer compartment (by determining minimum evaporator capacity) and performance characterization. Beyond the initial prototype, improvement in performance and energy efficiency of the RHX will be achieved with an optimized impeller design (which has lower mass), selection of a high-efficiency motor, lower fridge interior heating and improved chamber sealing. In addition, the promise of the RHX lies in its compactness and potential for utilization of collected frost in compressor subcooling.

The highest recovery rates were achieved in experiments 1 and 2, although the heat loss rate was 30% higher for experiment 1 vs. experiment 2. The reason for this was the constantly rotating impellers, which resulted in a higher continuous air flow (and thus heat transport) out of the insulated box through existing air exfiltration. Forced convection near the interior wall surfaces due to air circulation from the rotating impellers was also partially responsible for heat loss from the chamber. This condition persisted even when the compressor was off. This was not the case in experiment 2, since the impeller rotation cycled on and off along with the compressor. As the test chamber was warming from -21°C to -19°C with the compressor off, the air was stationary (with the exception of air circulation via buoyancy-induced natural convection) and air exfiltration out of the insulated box was lower as a result. For all experiments, the evaporator capacity (Q_{in}) was above 100 W, which met the requirements of a typical household freezer evaporator.

The power consumption of the compressor was also quantified and is shown below in Figure 5. This is important for household refrigeration applications since the compressor typically draws the majority of the power, with the exception of the defrost heater.

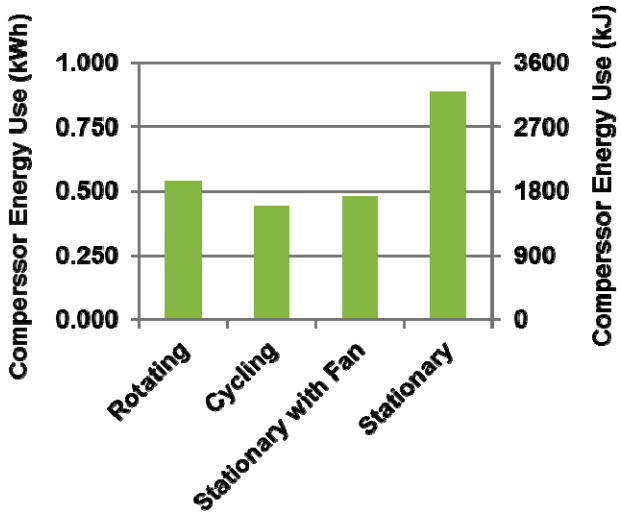

Figure 5: Compressor energy use for all experiments

The above results in Table 2 and Figure 5 indicate that although the COP for experiment 2 was only 4.3% higher than that of test 4, the energy consumed by the compressor in the refrigeration cycle was lower by 50.1%. As mentioned above, the reason for this was that the impellers produced significant air circulation with minimal frost formation, which allowed the evaporator capacity to increase and a lower chamber temperature setpoint to be reached. The compressor cycled on and off as a result (as did the impellers). It was only on for 51% of the time in a given cycle, leading to a lower overall energy consumption. It is important to note that the data in Table 2 and Figure 5 are steady-state measurements that do not reflect performance or energy consumption during periods of defrost. They illustrate the performance of the RHX system for different configurations, and comparisons to existing fin and tube evaporators currently used in household freezers will be made in future studies.

In addition to the performance study, a preliminary examination of the frost behavior on the RHX fins was conducted and used to elucidate the potential defrost energy savings for each operating condition. Images of frost formation on the impeller fins were captured during separate individual experiments which lasted longer than 24 hrs. However, all the same parameters (refrigerant mass flow rate, ambient conditions, impeller rotation speed) from the performance characterization studies above were maintained for the frost studies. Out of these, the most pertinent comparison was between the cycling and stationary impeller experiments (corresponding to experiments 2 and 4 above). Figure 6 shows the fin surfaces before and after a minimum of 24 hours had passed for the cycling and stationary impeller experiments. Figure 6(a.) is representative of both the cycling and stationary impeller cases at time 0:00.

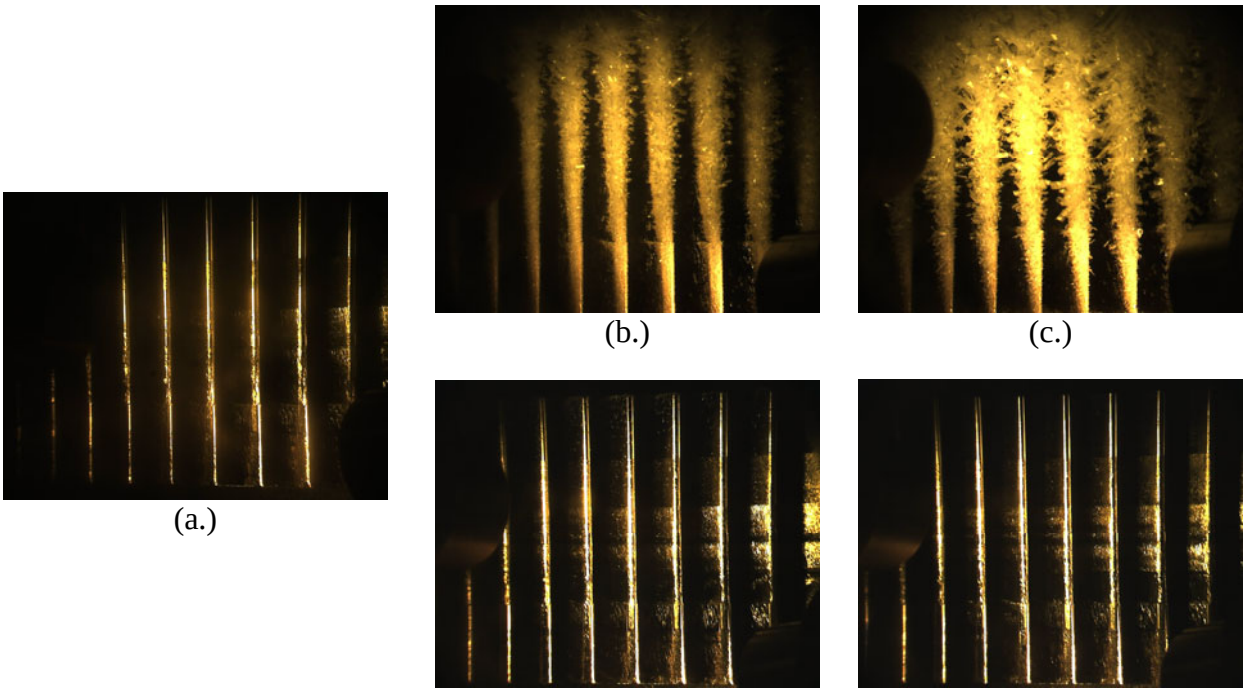

Figure 6: Images of frost formation on impeller fins for stationary and cycling experiments: (a.) hour 0:00 | (b.) hour 23:30, stationary impellers | (c.) hour 53.14, stationary impellers | (d.) hour 27:12, cycling impellers | (e.) hour 49:16, cycling impellers

The above results indicate that frost formation was minimal for the cycling impeller case, even after 49 hours of operation. By contrast, the fins in the stationary impeller experiment had significant layers of frost after 23 hours of operation. As mentioned above, the reason for the lack of frost formation in the cycling impeller experiment is due to the inherent operation of the rotating heat exchanger. High local air velocity in the vicinity of the fins during rotation inhibits the frost growth. The preliminary images and data show that the frequency of defrost cycles would be reduced by as much as 50% for the cycling impellers compared to the stationary impellers. This would result in 50% further energy savings related to defrosting, in addition to the savings achieved above, related to compressor cycling, for the RHX evaporator.

The results indicate that the optimum operating condition for the rotating heat exchanger acting as an evaporator is a cycling system in terms of performance and frost growth. With the optimum condition identified, further research efforts will focus on comparing it to that of a typical evaporator to compare similar metrics.

Conclusion

The performance characterization and frost study presented in this paper demonstrated the viability of using a rotating heat exchanger to replace current fin and tube heat exchanger design in residential refrigeration. The results showed that the RHX can meet the required capacity of a typical refrigerator (100W). The experiment involving cycling impellers alongside compressor power to maintain a chamber temperature of -20°C provided highest energy savings of 50.1% compared to the stationary impeller case. Also, the need to activate the defrost heaters

can be reduced, by using a rotating heat exchanger compared to a stationary one. The experimental data presented in this paper are part of a larger research study on frost growth on rotating surfaces.

Acknowledgments

This work was sponsored by the U. S. Department of Energy's Building Technologies Office under Contract No. DE-AC05-00OR22725 with UT-Battelle, LLC. The authors would also like to acknowledge Mr. Antonio Bouza, Technology Manager – HVAC&R, Water Heating, and Appliance, U.S. Department of Energy Building Technologies Office.

References

Cui, J., Li, W. Z., Liu, Y., Zhao, Y. S. 2011. "A new model for predicting performance of fin-and-tube heat exchanger under frost condition." International Journal of Heat and Fluid Flow. 32:1, 249-260. http://dx.doi.org/10.1016/j.ijheatfluidflow.2010.11.004.

da Silva, D. L., Hermes, C. J. L., and Melo, C. 2011. "Experimental study of frost accumulation on fan-supplied tube-fin evaporators." Applied Thermal Engineering, 31, 6–7:1013-1020. http://dx.doi.org/10.1016/j.applthermaleng.2010.11.006.

DOE (US Department of Energy). 2012. Standards. 77 Fed. Reg. 32308 (May 31).

EIA (Energy Information Administration). 2009. Residential Energy Consumption Survey (RECS). 2009 RECS Survey Data. http://www.eia.gov/consumption/residential/data/2009/.

Hwang, J., and Cho, K. 2014. "Numerical prediction of frost properties and performance of fin–tube heat exchanger with plain fin under frosting." International Journal of Refrigeration. 46, 59-68. http://dx.doi.org/10.1016/j.ijrefrig.2014.04.026.

Johnson, T. A., Koplow, J., Staats, W., Curgus, D., Leick, M., Matthew, D. et al. 2013. Development of the Sandia Cooler. Albuquerque, New Mexico 87185 and Livermore, California 94550: Sandia National Laboratories.

Knabben, F. T., Hermes, C. S., and Melo, C. 2011. "In-situ study of frosting and defrosting processes in tube-fin evaporators of household refrigerating appliances." International Journal of Refrigeration, 34.8: 2031-2041.

Lemmon, E.W., Huber, M.L., McLinden, M.O. 2013. *NIST Standard Reference Database 23: Reference Fluid Thermodynamic and Transport Properties-REFPROP, Version 9.1*, National Institute of Standards and Technology, Standard Reference Data Program, Gaithersburg MD.

Mauer, J., A. deLaski, S. Nadel, A. Fryer, and R. Young. 2013. Better Appliances: An Analysis of Performance, Features, and Price as Efficiency Has Improved. Washington, DC: ACEEE. http://aceee.org/research-report/a132.

Staats, W., Matthew, N., Hecht, E., Johnson, T., and Koplow, J. 2014. "Heat Transfer and Pressure Drop Performance of the Air Bearing Heat Exchanger." New York: ASHRAE.

York, D., Nadel, S., Rogers, E., Cluett, R., Kwatra, S., Sachs, H., Amann, J., and Kelly, M. 2015. New Horizons for Energy Efficiency: Major Opportunities to Reach Higher Electricity Savings by 2030. Washington, DC: ACEEE.